4406 *Macromolecules* **2001,** *34,* 4406−4415

On the Connection between Microstructure and Kinetics of (Pseudo)copolymerization†

Guglielmo Monaco

Dipartimento di Chimica, Università di Salerno, Via S.Allende, I-84081 Baronissi (SA), Italy

Received November 30, 2000; Revised Manuscript Received March 13, 2001

ABSTRACT: The connection between microstructure and kinetics in the case of irreversible growth of long (pseudo)copolymers has been discussed, extended and established. The theoretical results have been cast in simple matrix equations which enable one to compute the probability to find any given sequence in terms of ratios of kinetic constants, rather than in terms of stochastic parameters. As an application, the case of regioregular polymerization of vinyl monomers by C_1-symmetric coordination catalysts has been considered. In addition to propagation, first order in monomer concentration, chain and site epimerization, both zeroth-order in monomer concentration, have been taken into account. The resulting equations have been tested against a set of literature data obtained by five different catalysts, each operated at five different concentrations, resulting in the evaluation of ratios of kinetic constants. For all catalysts the quantitative analysis of the kinetics confirms that the contribution of chain epimerization is small or negligible in the concentration range examined.

Introduction

Microstructure is the result of the balance of all the processes occurring during the growth of the polymer chain and thus its analysis can give precious information about (pseudo)copolymerization[1] mechanisms.[3] However, general connections between microstructure and kinetics of (pseudo)copolymerization are often cast in terms of rather complicated mathematical expressions,[4,5] and as a matter of fact, the analysis of microstructural data is more often based on pure statistics rather than kinetics.[6−9]

The continuous development of new pseudo-copolymerization catalysts,[10−12] the increase of quality and quantity of microstructural data, mainly due to the adoption of ^{13}C NMR spectroscopy,[13,14] and the present possibility to investigate by computational approaches rather complicated kinetic models[15] call for an assessment of this topic. It is the purpose of this paper to discuss, establish, and extend the connection between microstructure and kinetics of (pseudo)copolymerization in the case of irreversible growth of long polymer chains.

The theoretical solutions, which will be discussed, present the advantage to be cast in matrix equations, thus enabling fast computations of microstructural data.

As an application, the general theory will be specialized to regioregular polymerization of vinyl monomers by a C_1-symmetric coordination catalyst allowing chain and site epimerization. The resulting equations will then be applied to a set of microstructural data obtained from C_s and C_1 zirconocene catalysts.[16]

Theory

Basic Notation and Preliminary Considerations. A linear (pseudo)copolymer can be described by a string of M symbols identifying different units U_1, U_2, ..., U_M, which derive from one or more monomers, depending on if we deal with a pseudo-copolymer or a true copolymer.[1] The microstructure of linear (pseudo)copolymers is often analyzed in terms of Markov models Mm,[17] which assume that the probability to find a given unit U_j in a long chain depends on the kinds of no more than m preceding units.[18] A sequence of m units can be found in M^m microstructural states s_1, s_2, ..., s_{M^m}. Then the key quantities of a Markov model Mm are the $M^m \times M^m$ conditional probabilities $T(s_i \rightarrow s_j)$ of finding the microstructural state s_j after the microstructural state s_i. These probabilities define the transition matrix $\mathbf{T}$.[19]

Using an Mm model of sufficiently high order, it is always possible to reproduce the microstructure of a single (pseudo)copolymer.[3] On the other hand, it is well-known that the microstructure of copolymers depends on the ratio(s) of monomer concentrations in the feed.[20] Moreover microstructural dependence on monomer concentration can also be found for pseudo-copolymerization catalysts.[16,21−23] In these cases the parameters of an Mm model are not of great use in that they are not reasonably tranferable to polymers produced with the same catalytic system but with different monomer concentration(s). Transferable parameters could only be obtained if one succeeded in interpreting the microstructure in terms of the kinetic model of the pseudo-copolymerization in exam.

It must be noted that microstructural analyses are not standard kinetic studies; indeed, they are not based on measurements of any time-dependent observable quantity. Therefore, they cannot lead to the evaluation of the absolute velocity of any process. A more relevant problem is found when the information carried by the microstructural states is incomplete in the framework of a kinetic model of polymerization. As an example, if we consider a catalyst oscillating between two distinguishable forms, the observation of unit U_j does not bear information on the form of the catalyst which was responsible of its polymerization. In similar cases, it has been proposed to interpret the microstructure in terms of Markov chains built over the states which are relevant to the kinetic model in exam, rather than over the microstructural states.[15,24,25] Hereafter, these "kinetic states" and their transition matrix will be labeled by over barred symbols: $\bar{s}_i$ and $\bar{\mathbf{T}}$.

---

† A preliminary account of this paper was presented at the third workshop on "Advances on Insertion Polymerization", Ischia (NA), Italy, 11−13 Sept, 2000.

10.1021/ma002044y CCC: $20.00

The development of Markov models in the space of kinetic states can be rather successful; but it should be recognized that the stochastic parameters needed to set up the transition matrix cannot be interpreted in terms of kinetic constants until their parent kinetic scheme is solved. This has been done long ago[26,27] in the case of a well-known reference model for copolymerization.[20] Aiming at generalizing the latter model, we will restate its main assumptions as follows.

(1) There is a large number of growing chains in an homogeneous environment with constant pressure, temperature, and monomer concentrations in the feed. Each chain grows independently of the other chains.

Therefore, the kinetics is defined by the evolution of a single chain averaged over the ensemble.

(2) Depolymerization is forbidden.

This implies that one can consider the (pseudo)copolymerization process as a sequence of growth events

$$...\bar{s}_i^{n-1} \longrightarrow \bar{s}_j{}^n,\ \bar{s}_j{}^n \longrightarrow \bar{s}_k^{n+1}...$$

where $\bar{s}_j{}^n$ indicates that the chain is found in state j immediately after the insertion of the nth monomer.

The conditional probabilities $\bar{T}_{ij}^{(n)}$ to obtain state $\bar{s}_j{}^n$ starting from state $\bar{s}_i^{n-1}$ define the transition matrix $\bar{\mathbf{T}}^{(n)}$.

(3) All the kinetic constants are assumed to be independent of chain length, namely the transition matrix $\bar{\mathbf{T}}$ is independent of n.

Therefore, after averaging over the ensemble, all the steps of chain lengthening will be equal and we can focus on the general step of chain lengthening from n to $n + 1$ units.

We will have $2N$ accessible states

$$\{\bar{s}_1^n, \bar{s}_2^n ... \bar{s}_N^n, \bar{s}_1^{n+1}, \bar{s}_2^{n+1} ... \bar{s}_N^{n+1}\} \equiv \{\bar{\mathbf{s}}^n, \bar{\mathbf{s}}^{n+1}\} \equiv \bar{\mathbf{s}}$$

where the vectors $\bar{\mathbf{s}}^n$, $\bar{\mathbf{s}}^{n+1}$, and $\bar{\mathbf{s}}$ are formed by symbols of states.

(4) All states are completely defined after identification of the last m inserted unit(s).

This means that the states of the kinetic model are in a one-to-one correspondence with the states of an mth order Markov model.

(5) Any transformation of short states ($\bar{s}_i^n \rightarrow \bar{s}_j^n$) is forbidden.

According to this model, the transition matrices $\bar{\mathbf{T}}$ and $\mathbf{T}$ coincide, with

$$T_{ij} = w(\bar{s}_i^n \rightarrow \bar{s}_j^{n+1}) \sum_k w(\bar{s}_i^n \rightarrow \bar{s}_k^{n+1}) \qquad (1)$$

where $w(\bar{s}_i^n \rightarrow \bar{s}_j^{n+1})$ is the transition probability per unit time from state $\bar{s}_i^n$ to state $\bar{s}_j^{n+1}$ and can be expressed in terms of monomer concentrations and kinetic constants.[20] In this case experimental evidences in favor of an mth order Markovian model Mm are an indication that the kinetic constants of propagation are sensitive to the nature of m preceding units.

However, as will be discussed in the next paragraph, such a nice correspondence is no longer found when assumption 4 and/or assumption 5 break down.

(b4) Given a sequence of last inserted units, the catalyst can be present in several thermally accessible states with distinguishable catalytic properties, leading to more "kinetic states" than "microstructural states";

(b5) One is faced with oscillating catalysts and/or with rearrangement of the growing chain.[28]

If only assumption 4 breaks down, the observed microstructure is a weighted average of different microstructures,[9,29] while if both assumptions 4 and 5 break down, the interpretation of the microstructure is not so straightforward.

Coleman and Fox were the first to consider from a kinetic point of view a case of breakdown of assumptions 4 and 5 in the analysis of polymerization of vinyl monomers.[30] They derived expressions for the microstructure obtained by oscillating catalysts in terms of monomer concentration and ratios of the kinetic constants of the model; moreover they also derived a useful matrix multiplication technique enabling fast computation of the microstructure.

In their model, the kinetic states were dyads rather than units. This choice turns out to be correct as far as a Bovey or chain-end propagation model[31] is assumed—as they did. However it also constitutes a limitation in the analysis of more involved stereochemical models, where an explicit indication of the units is mandatory.[15,24,25] Moreover they did not consider the case of chain rearrangements, which are found in many situations such as the polymerization of ethylene, where the growing chain can undergo several reactions leading to the formation of side branches,[32] or the coordination polymerization of α-olefins, where considerable rearrangements of the last units of the chain are possible.[11,23] In these cases the rearrangements cancel out a piece of microstructure already "written" by previous propagation reactions.

In the following paragraph, we will tackle the problem of establishing the general connection between kinetics and microstructure for a kinetic model which has no requirements beyond assumptions 1–3.

General Formulation. Assumption 1 implies that, according to the standard chemical approach to the kinetics, the general step of growth $\bar{\mathbf{s}}^n \rightarrow \bar{\mathbf{s}}^{n+1}$ can be described in terms of a set of linear differential equations describing the velocity of variation of the $2N$ concentrations C_i of chains in the states $\{\bar{\mathbf{s}}^n, \bar{\mathbf{s}}^{n+1}\}$. However absolute concentrations of the kinetic states are inaccessible and irrelevant in microstructural investigations and the standard kinetic equations should be normalized in order to get the $2N$ probabilities $p_i = C_i / \sum_{j=1}^{2N} C_j$, which will be grouped in the row vector $\mathbf{p} = [\mathbf{p}^n\ \mathbf{p}^{n+1}]$.

Thus, one gets the master equation[19,33]

$$\mathrm{d}\mathbf{p}/\mathrm{d}t = \mathbf{p}\mathbf{W} \qquad (2)$$

where the elements of the evolution matrix $\mathbf{W}$ are given by $W_{i \neq j} = w_{ij}$ and $W_{ii} = -\sum_j w_{ij}$ and w_{ij} is the transition probability per unit time from state $\bar{s}_i$ to $\bar{s}_j$.

The solution of the master equation enables to compute at any time $t > 0$ the probability $p_i(t)$ to find the system in any state $\bar{s}_i$.

According to assumption 2 of irreversible growth, the evolution matrix $\mathbf{W}$ has the following structure:

$$\mathbf{W} = \begin{array}{c|cc} & \mathbf{s}^n & \mathbf{s}^{n+1} \\ \hline \mathbf{s}^n & \mathbf{W}^{int} & \mathbf{W}^{gr} \\ \mathbf{s}^{n+1} & \mathbf{0} & \mathbf{0} \end{array} \qquad (3)$$

where the apices int and gr remind one that the extradiagonal elements of the submatrices $\mathbf{W}^{\mathrm{int}}$ and $\mathbf{W}^{\mathrm{gr}}$

describe interconversion of n-unit states ($\bar{s}_i^n \rightarrow \bar{s}_j^n$) and growth ($\bar{s}_i^n \rightarrow \bar{s}_j^{n+1}$), respectively.

With such a peculiar structure of the evolution matrix (eq 3), the master equation can be reduced to the following two equations:

$$\mathrm{d}\mathbf{p}^n/\mathrm{d}t = \mathbf{p}^n\mathbf{W}^{\mathrm{int}} \tag{4}$$

$$\mathrm{d}\mathbf{p}^{n+1}/\mathrm{d}t = \mathbf{p}^n\mathbf{W}^{\mathrm{gr}} \tag{5}$$

The solution of eq 4 is

$$\mathbf{p}^n(t) = \mathbf{p}^n(0)\exp(\mathbf{W}^{\mathrm{int}}t) \tag{6}$$

The stationary evolution of the system rests well-defined if one knows the probabilities $p_k^{n+1}(\infty)$ to be in state $\bar{s}_k^{n+1}$ starting from a system in state $\bar{s}_i^n$, i.e. $p_i^n(0) = 1$. The probabilities $p_k^{n+1}(\infty)$ will be the probabilities $p_k^{n+1}(0)$ in the computation of the successive insertion ($\bar{s}_i^{n+1} \rightarrow \bar{s}_j^{n+2}$). It will be convenient to introduce the matrices $\bar{\mathbf{T}}^-(t)$ and $\bar{\mathbf{T}}^+(t)$, whose ijth elements are the solutions $p_j^n(t)$ and $p_j^{n+1}(t)$ obtained when the system was initially in state $\bar{s}_i^{n+1}$ ($\bar{\mathbf{T}}^-(0)$ is the identity matrix). Substituting eq 6 into eq 5, one gets

$$\bar{\mathbf{T}} = \lim_{t\rightarrow\infty}\bar{\mathbf{T}}^+(t) = \lim_{t\rightarrow\infty}\int_0^t \bar{\mathbf{T}}^-\mathbf{W}^{\mathrm{gr}}\,\mathrm{d}t' = \left(\lim_{t\rightarrow\infty}\int_0^t \exp(\mathbf{W}^{\mathrm{int}}t')\,\mathrm{d}t'\right)\mathbf{W}^{\mathrm{gr}} \tag{7}$$

Under hypothesis 2 of an irreversible growth (which translates into the mathematical condition $\lim_{t\rightarrow\infty}\exp(\mathbf{W}^{\mathrm{int}}t) = 0$), one gets the elegant result

$$\bar{\mathbf{T}} = -(\mathbf{W}^{\mathrm{int}})^{-1}\mathbf{W}^{\mathrm{gr}} \tag{8}$$

Equation 8 reveals that the matrix $\bar{\mathbf{T}}$ is unchanged by a change of speed of all the processes, which can be described by the transformations $\mathbf{W}^{\mathrm{int}} \rightarrow \boldsymbol{\tau}\mathbf{W}^{\mathrm{int}}$, $\mathbf{W}^{\mathrm{gr}} \rightarrow \boldsymbol{\tau}\mathbf{W}^{\mathrm{gr}}$, where $\boldsymbol{\tau}$ is an arbitrarily chosen diagonal matrix. This corresponds to the impossibility of retrieving absolute velocities from microstructural analyses. From an operational point of view, it can be convenient to chose a $\boldsymbol{\tau}$ matrix which renders each diagonal element $\mathbf{W}^{\mathrm{int}}$ equal to -1, i.e. $\tau_{ij} = \delta_{ij}/\sum_k w(\bar{s}_i^{n+1} \rightarrow \bar{s}_k^{n+1})$. It can be checked that, upon validity of assumptions 4−5, eq 8 gives the familiar result 1.

The matrix $\bar{\mathbf{T}}$ is stochastic and computation of the row vector $\mathbf{p}^\infty$ of its stationary probabilities can be performed in the usual manner.[19] The probability to have any sequence of kinetic states can be computed in a straightforward manner; e.g., the probability to have the sequence $\bar{s}_i^{n+1}\ \bar{s}_j^{n+2}\ \bar{s}_k^{n+3}$ will be

$$p(\bar{s}_i^{n+1}\ \bar{s}_j^{n+2}\ \bar{s}_k^{n+3}) = p_i^\infty \bar{T}_{ij}\bar{T}_{jk} \tag{9}$$

On the other hand, to compute the probability of any sequence of units, we need to sum over all sequences of kinetic states which correspond to that sequence of units. To this end it is convenient to define a matrix $\boldsymbol{\Phi}$ of dimensions $N \times N$, such that all of its rows are equal to $\mathbf{p}^\infty$, or a row vector $\mathbf{J}$ of length N composed by all ones. According to this notation and when the order m of the Markov chain over the kinetic states exceeds the number L of last inserted units allowed to rearrange,[28] the probability of obtaining any sequence of units can be obtained by a matrix generalization of eq 9; e.g., for the microstructural sequence $U_iU_jU_k$, we get

$$p(U_iU_jU_k) = \mathrm{Tr}(\boldsymbol{\Phi}_i\bar{\mathbf{T}}_j\bar{\mathbf{T}}_k) = \mathbf{p}_i^\infty\bar{\mathbf{T}}_j\bar{\mathbf{T}}_k\mathbf{J}^T \tag{10}$$

where the apex T indicates transposition and the subscript $i \in [1,M]$ indicates that only the columns referring to the kinetic states in correspondence to the microstructural state U_i are retained, while the remaining columns are set to zero.

To have a computed microstructure which follows an mth order Markov chain, for any sequence $U_iU_j \ldots U_pU_q$ composed by more than $m + 1$ units the ratio $\mathrm{Tr}(\boldsymbol{\Phi}_i\bar{\mathbf{T}}_j \ldots \bar{\mathbf{T}}_p\bar{\mathbf{T}}_q)/\mathrm{Tr}(\boldsymbol{\Phi}_i\bar{\mathbf{T}}_j \ldots \bar{\mathbf{T}}_p)$ should be independent of the length of the sequence.[30] This strict condition turns out to be verified when all of the nonzero elements of the $\boldsymbol{\Phi}_i\bar{\mathbf{T}}_j \ldots \bar{\mathbf{T}}_p$ matrix are equal. Apart from exceptional cases, this condition is met only when there is a single nonzero element in the quoted matrix, which happens when there is a one-to-one correspondence between microstructural and kinetic states. In the more general case of failure of assumption 4, the above ratio is generally dependent on the nature of the preceding units, whichever value of m is chosen: the chain is non-Markovian.[18,20,30,34] This is just a chemical example of a hidden Markov chain,[35] a chain which satisfies the Markov property when described in a proper space (that of the states of the kinetic model) but loses this property when projected on a different space (that of observable microstructural states).

In this situation, one should agree with Price:[6] a description of the microstructure in terms of Markov chains (built over microstructural states) does not bear any information on kinetics.

Nevertheless, when a kinetic model following assumptions 1−3 is defined, eqs 8 and 10 form a sound bridge between kinetics and microstructure, thus allowing the determination of ratios of kinetic constants starting from microstructural data.

From an operational point of view, if one has determined a set of independent fractional abundances p_i^{exp} of sequences obtained under well-defined experimental conditions together with reasonable statistical estimates σ_i of the uncertainty on their values, the best values of the parameters of a given kinetic model can be obtained by minimization of the goodness of fit indicator

$$\chi_r^2 = \sum_i \frac{(p_i^{\mathrm{exp}} - p_i)^2}{\nu\sigma_i^2} \tag{11}$$

where the computed probabilities p_i are given by eq 10 and the number ν of degrees of freedom is given by the difference between independent data and adjustable parameters. We remind that, when one compares a set of different kinetic models, the one with χ_r^2 closer to one is statistically more likely.

The Case of Regioregular Vinyl Polymerization by *C*$_1$-Symmetric Catalysts. For a regioregular vinyl polymer growing on an active site, its tertiary carbon atoms will be chiral and can be safely labeled as R or S, according to the standard stereochemical nomenclature.[36] Thus, a growing polymer chain can be depicted as a string of R and S letters.

However, from a kinetic point of view, the situation is not so simple. Indeed, a coordination catalyst needs at least two coordination positions, one for the incoming monomer and one for the growing chain, and if the two

Scheme 1

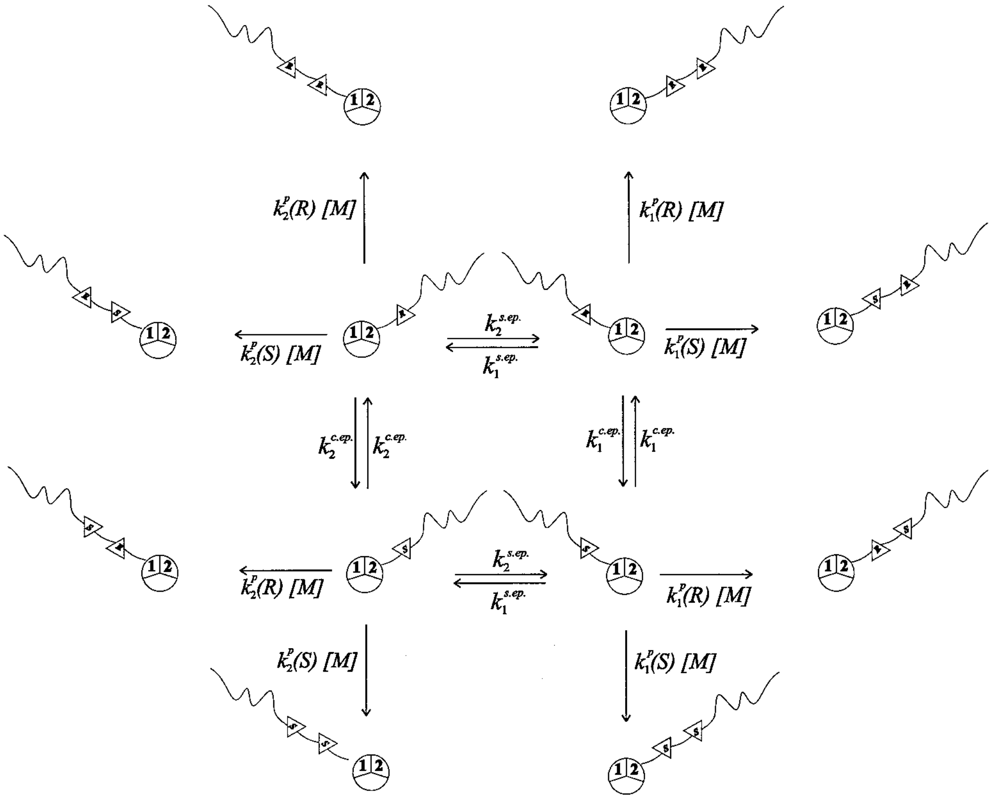

coordination positions are not homotopic and can be occupied by both chain and monomer, the specification of the type of the last (or last few) inserted units is insufficient to characterize the kinetic states. In this situation for a chain of x units ($x = n$, $n + 1$), one should use at least four kinetic states $\{R_1^x, S_1^x, R_2^x, S_2^x\} \equiv \{\{1^x\}, \{2^x\}\}$, where the symbol R_1^x (S_1^x) indicates a state with a chain coordinated in position i with the last inserted unit of chirality R (S).

Available experimental and computational results[37-40] confirm Cossee's hypothesis[41] that upon insertion of a vinyl monomer the chain changes the position of coordination. In effect, it is this mechanism of chain migratory insertion which allows one to produce syndiotactic polymers by catalysts with enantiotopic coordination positions.[21]

For coordination catalysts, beside insertion, two other reactions have been proposed, which occur in the absence of the monomer. The first one (site epimerization, also named back skip) consists in the jump of the chain form position 1 to position 2 (and vice versa), while the second (chain epimerization) consists in the change of chirality of the last inserted unit.[11]

We will assume that all the kinetic constants of the above reactions do not depend on the chirality of the last inserted unit, although more general cases[9,42] can be considered rather easily. As far as the insertion reaction is concerned, such an assumption is usually referred in the field of polymer science as "enantiomorphic sites" model, a reference starting point for the description of the polymer produced by a chiral active site.[43] Moreover, the insertion reaction will be assumed to be first order in monomer concentration, which corresponds[11] to the predominance of one insertion path out of the different paths, which can arise for different conformations of the growing chain.[37]

The possibility of chain epimerization implies that the chirality of the last inserted tertiary carbon is not definitely established until a new monomer is inserted, and thus, for a kinetic model to have a correspondence with observed microstructure, the kinetic states should specify also the next to the last inserted unit.[28] Thus, for a chain of x units ($x = n$, $n + 1$), one should use eight states:

$$\{RR_1^x, RS_1^x, RR_2^x, RS_2^x, SR_1^x, SS_1^x, SR_2^x, SS_2^x\} \equiv \{\{R1^x\}, \{R2^x\}, \{S1^x\}, \{S2^x\}\} \equiv \{\{R\bullet^x\}, \{S\bullet^x\}\}$$

The resulting kinetic model is sketched in Scheme 1, where R and S chiralities are distinguished by up and down triangles and the apices p, c.ep., and s.ep. indicate propagation and chain and site epimerizations, respectively.

Because of the competition between reactions of different order in monomer concentration, the microstructure obtained according to Scheme 1 is expected to depend significantly upon monomer concentration, a fact which has been verified in several cases.[16,21-23,44]

In the presence of significant chain epimerization, the tacticity of the polymer is expected to decrease with monomer concentration.

This situation has been unambiguously verified in the case of enantioselective C_2-symmetric catalysts.[23]

On the other hand the decrease of tacticity with monomer concentration observed in C_s-symmetric systems could arise from both site and chain epimerization. The main role of site epimerization has been demonstrated by use of deuterated monomers in the case of a doubly bridged C_s-symmetric catalyst.[16]

Still a different situation is observed for some C_1-symmetric systems, which show a significant increase of isotacticity when decreasing monomer concentra-

Table 1. Results Obtained from the Least-Squares Analysis of Pentad Percentages of Polypropylenes Obtained by C_s-Symmetric Catalysts 1a–c Operated at Room Temperature and in Toluene Solution at Five Different Monomer Concentrations: $[C_3H_6]$ = 0.8, 1.5, 2.1, 2.8, 3.4 M for Catalysts 1a and 1c and $[C_3H_6]$ = 0.8, 1.5, 2.1, 2.9, and 3.4 M for Catalyst 1b[a]

	best-fit parameters			
exptl information from ref 16	$\bar{k}_1^{\text{c.ep.}}$ (M)	$\bar{k}^{\text{s.ep.}}$ (M)	σ^{R}	goodness of fit
R = H (catalyst **1a**)	0.013 ± 0.002	0.068 ± 0.002	0.9952 ± 0.0011	$0.6 < \chi_r^2 < 2.5$
$3 \times 10^4 < M_w < 1 \times 10^5$	0 (fixed)	0.0713 ± 0.0015	0.9893 ± 0.0012	$0.7 < \chi_r^2 < 2.7$
$0.906 < r < 0.971$				
21 independent data				
R = CH(Me$_2$) (catalyst **1b**)	0.014 ± 0.007	0.151 ± 0.009	0.993 ± 0.002	$2.8 < \chi_r^2 < 11.3$
$3 \times 10^4 < M_w < 2 \times 10^5$	0 (fixed)	0.186 ± 0.004	1.000 ± 0.003	$2.4 < \chi_r^2 < 9.5$
$0.802 < r < 0.971$				
23 independent data				
R = SiMe$_3$ (catalyst **1c**)	0.017 ± 0.002	0.196 ± 0.003	1.0000 ± 0.0011	$0.5 < \chi_r^2 < 1.9$
$4 \times 10^4 < M_w < 1 \times 10^5$	0 (fixed)	0.204 ± 0.002	0.9939 ± 0.0012	$0.5 < \chi_r^2 < 2.0$
$0.815 < r < 0.965$				
27 independent data				

[a] Errors correspond to the 95% confidence interval for each parameter.

tion.[22,44] This behavior, ascribed to chain back skip to the lower energy more enantioselective position,[45] indicates that the chain epimerization reaction should be of negligible importance.

Nevertheless, it cannot be excluded that chain epimerization can be relevant in different systems, particularly in C_1-symmetric systems which do not show a considerable increase of tacticity when lowering the concentration. Therefore, not only a general solution of Scheme 1 is a complete example of the kinetic scheme described above (because it considers both an “oscillating” catalyst and chain rearrangements), but it can also be expected to help in the analysis of microstructural data obtained from known and future catalysts.

The complete setup of the evolution matrices is given in the Appendix. At a given monomer concentration, the microstructure rests defined by the six ratios of kinetic constants:

$$\bar{k}_x^{\text{c.ep.}} = k_x^{\text{c.ep.}}/k_x^{\text{p}}, \quad \bar{k}_x^{\text{s.ep.}} = k_x^{\text{s.ep.}}/k_x^{\text{p}}, \quad \sigma_x = k_x^{\text{p}}(R)/k_x^{\text{p}} \qquad (12)$$

where the subscript $x = 1,2$ indicates the position occupied by the chain before the epimerization or the insertion and $k_x^{\text{p}} = k_x^{\text{p}}(R) + k_x^{\text{p}}(S)$.

For C_2-symmetric catalysts, the parameters of position 1 should be equal to those of position 2. This should also be the case for C_s-symmetric catalysts, except that σ_1 is expected to be equal to $1 - \sigma_2$, due to the enantiotopicity of the two coordination positions.

It should be considered that NMR data give information about dyads (usually indicated according to the Bovey *m*/*r* notation[20,46]) and not units (*R*/*S*). This implies that the same microstructural data are obtained changing σ_x with $(1 - \sigma_x)$ for both positions.[43] Although this indetermination prevents one from getting information on the absolute chirality preferred at a given position, for a C_1-symmetric system it is still possible to have information about the relative chirality preferred at the two sites; depending on if the signs of $(\sigma_1 - 0.5)$ and $(\sigma_2 - 0.5)$ are different or equal, one has the point that opposite or identical chiralities are preferred at the two positions.

In the Appendix, the general solution has also been specialized in the case of absence of chain epimerization reaction, and the stochastic parameters needed for the interpretation of the microstructure have been expressed in terms of kinetic constants and monomer concentration. The probabilities $P_{xx} = 1 - P_{xy}$ that two consecutive insertions occur on the same position of the catalyst turn out to be

Chart 1

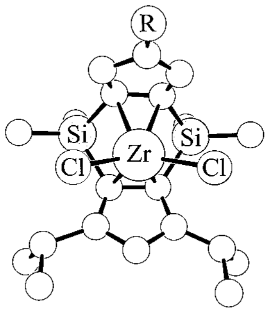

$$1 - P_{x \neq y} = \frac{\bar{k}_x^{\text{s.ep.}}}{\bar{k}_1^{\text{s.ep.}} + \bar{k}_2^{\text{s.ep.}} + [M]} \qquad (13)$$

Equations 13 can be easily recast in order to obtain the following linear relationships

$$\frac{P_{12}}{1 - P_{12}} = \frac{k_2^{\text{s.ep.}}\, k_1^{\text{p}}}{k_2^{\text{p}}\, k_1^{\text{s.ep.}}} + \frac{k_1^{\text{p}}}{k_1^{\text{s.ep.}}}[M] \qquad (14)$$

$$\frac{P_{21}}{1 - P_{21}} = \frac{k_1^{\text{s.ep.}}\, k_2^{\text{p}}}{k_1^{\text{p}}\, k_2^{\text{s.ep.}}} + \frac{k_2^{\text{p}}}{k_2^{\text{s.ep.}}}[M] \qquad (15)$$

It can be easily seen, either from eq 13 or from eqs 14 and 15 that as $[M] \rightarrow \infty$, i.e. when the site epimerization cannot disturb the regular alternation of the chain migratory mechanism, one correctly obtains $P_{12} = P_{21} = 1$.

On the other hand when $[M] \rightarrow 0$, one gets the result obtainable by imposing a preequilibrium between the two positions of coordination of the chain:

$$\frac{P_{12}}{1 - P_{12}} = \frac{1 - P_{21}}{P_{21}} = \frac{k_2^{\text{s.ep.}}\, k_1^{\text{p}}}{k_2^{\text{p}}\, k_1^{\text{s.ep.}}}$$

Results and Discussion

Experimental tests of the above kinetic scheme on the basis of microstructural data face with many chemical and analytical problems. Indeed in order to analyze a simple kinetic scheme, the catalytic system should be

Table 2. Results Obtained from the Least-Squares Analysis of Pentad Percentages of Polypropylenes Obtained by C_1-Symmetric Catalysts 1d−e Operated at Room Temperature and in Toluene Solution at Five Different Monomer Concentrations: $[C_3H_6] = 0.5, 0.8, 2.1, 3.4, 4.6$ M[a]

	best-fit parameters						
exptl information from ref 16	$\bar{k}_1^{c.ep.}$ (M)	$\bar{k}_1^{s.ep.}$ (M)	σ_1^R	$\bar{k}_2^{c.ep.}$ (M)	$\bar{k}_2^{s.ep.}$ (M)	σ_2^R	goodness of fit
R = *rac*-CH(Me)(CMe$_3$) (cat. **1d**)	0.003 ± 0.004	0.00± ± 0.04	1.000 ± 0.004	0.000 ± 0.004	6.8 ± 0.8	0.0 ± 0.2	$2.8 < \chi_r^2 < 11.1$
$2 \times 10^4 < M_w < 5 \times 10^4$	0.003 ± 0.004	0 (fixed)	1 (fixed)	0 (fixed)	6.8 ± 0.4	0.01 ± 0.19	$2.5 < \chi_r^2 < 10.0$
$0.115 < r < 0.633$	0 (fixed)	0 (fixed)	1 (fixed)	0 (fixed)	6.2 ± 0.4	0.05 ± 0.05	$2.4 < \chi_r^2 < 9.7$
32 independent data							
R = (1*R*,2*S*,5*R*)-menthyl (cat. **1e**)	0.0635 ± 0.0016	0.00 ± 0.02	1.000 ± 0.003	0.0000 ± 0.0009	1.53 ± 0.04	0.150 ± 0.006	$0.7 < \chi_r^2 < 2.9$
$4 \times 10^4 < M_w < 1 \times 10^5$	0.0636 ± 0.0014	0 (fixed)	1 (fixed)	0 (fixed)	1.54 ± 0.04	0.149 ± 0.004	$0.7 < \chi_r^2 < 2.7$
$0.403 < r < 0.745$	0 (fixed)	0 (fixed)	1 (fixed)	0 (fixed)	1.17 ± 0.03	0.192 ± 0.004	$1.0 < \chi_r^2 < 4.1$
40 independent data							

[a] Errors correspond to the 95% confidence interval for each parameter.

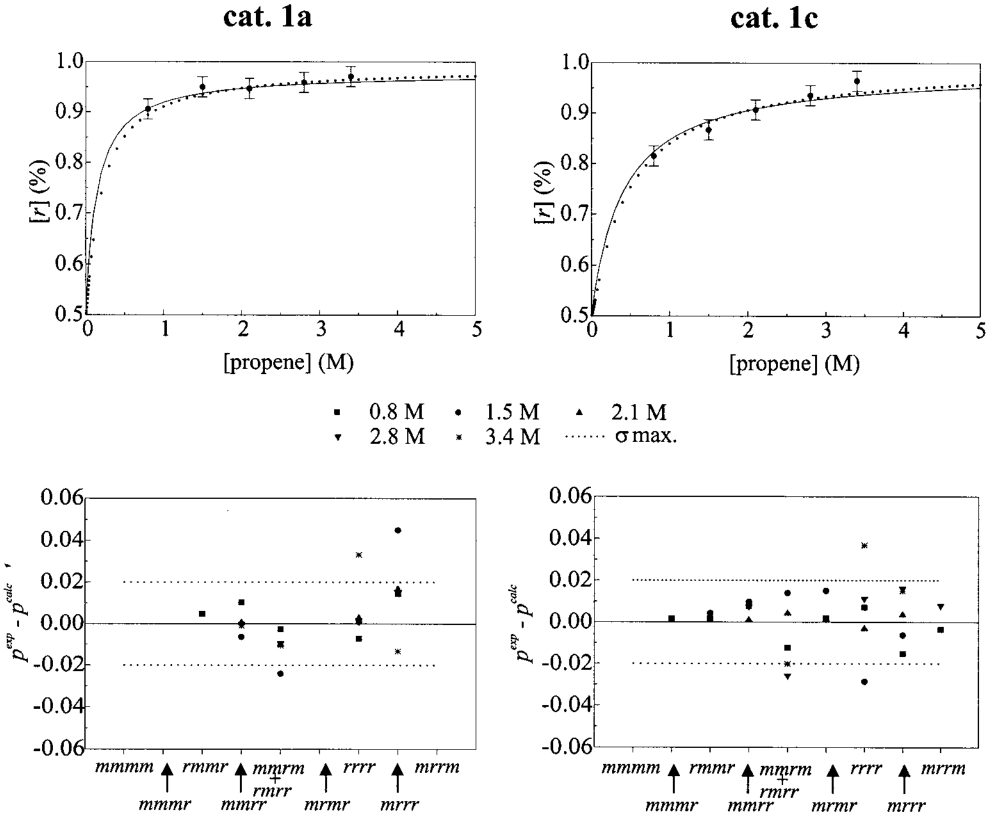

Figure 1. Top: plots of the theoretical dependence of the percentage of the *r* dyad upon monomer concentration. The lines have been obtained with the parameters reported in Table 1 for catalysts **1a** and **1c**. The continuous and dotted lines correspond, respectively, to zero and nonzero rate constant of chain epimerization $k^{c.ep.}$. The experimental points and the error bars[48] have been derived from ref 16. Bottom: plots of residuals obtained by fitting with two kinetic parameters the experimental percentages of pentads retrieved by the ^{13}C NMR analysis of five polypropylene samples produced by the C_s-symmetric catalysts **1a** and **1c** operated at five different monomer concentrations.[16]

as single-sited as possible and this is not always a simple matter, even for metallocene catalysts.[11] Moreover in order to quantitatively test a kinetic scheme according to eq 11, one should evaluate a sufficient number of percentages p_i^{exp} and their errors σ_i, which, despite well established spectroscopic procedures, remains a subtle point. As a matter of fact, microstructural studies which report error estimates σ_i can be safely considered to be the exception rather than the rule.[47]

Taking these warnings into account, we will now proceed to analyze the microstructural data obtained by five doubly silylene-bridged zirconocene catalysts reported in ref 16. The basic structure of the catalysts, shown in Chart 1, is $(1,2\text{-SiMe}_2)_2\{\eta^5\text{-C}_5\text{H}_2\text{-4-R}\}\{\eta^5\text{-C}_5\text{H-3,5-(CHMe}_2)_2\}\text{ZrCl}_2$. The five catalysts differ by the nature of the substituent: R = H (catalyst **1a**), *rac*-CHMe$_2$ (catalyst **1b**), SiMe$_3$ (catalyst **1c**), CHMe(CMe)$_3$ (catalyst **1d**), (1*R*,2*S*,5*R*)-menthyl (catalyst **1e**). According to the nature of the R group the catalysts have been classified as C_s- (**1a**−**c**) and C_1-symmetric (**1d**,**e**).

For each catalyst, we analyzed the five sets of pentad fractional abundances reported for polymerizations carried out at room temperature in toluene solution. Some additional experimental details can be found in Tables 1 and 2, while more complete information can be found in ref 16. Pentad fractional abundances p_i^{exp} lower than 0.010 were not reported, but we still had a considerable number of independent data ranging from 21 to 40 (Tables 1 and 2).

On the other hand the estimation of errors was lacking; only the reproducibility of the percentage $p(r)$ of the *r* dyad was studied and declared as ±0.02. Thus, any straightforward use of eq 11 was prevented, and

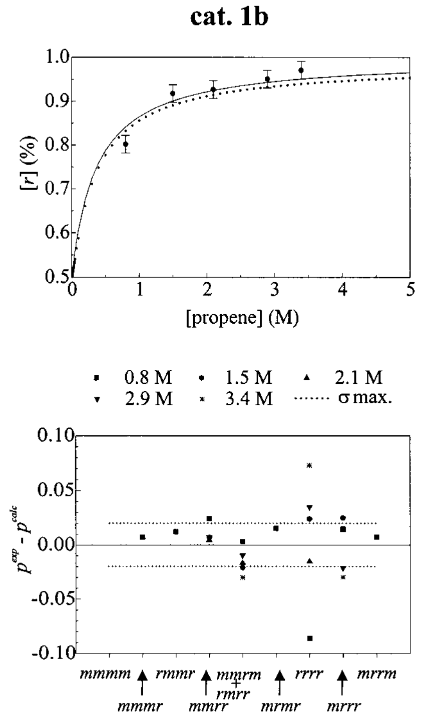

Figure 2. Top: plots of the theoretical dependence of the percentage of the *r* dyad upon monomer concentration. The lines have been obtained with the parameters reported in Table 1 for catalyst **1b**. The continuous and dotted line correspond, respectively, to zero and nonzero rate constant of chain epimerization $k^{c.ep.}$. The experimental points and the error bars[48] have been derived from ref 16. Bottom: plots of residuals obtained by fitting with two kinetic parameters the experimental percentages of pentads retrieved by the ^{13}C NMR analysis of five polypropylene samples produced by the C_s-symmetric catalyst **1b** operated at five different monomer concentrations.[16]

we were forced to a standard least squares refinement of the parameters of the models chosen to analyze the five sets of data.

Nevertheless a rough estimate of a lower and an upper bound for χ_r^2 can still be made, assuming equal errors $0.010 < \sigma < 0.02$ for all the data.[48]

***C_s*-Symmetric Systems.** To investigate in a quantitative manner the relevance of chain epimerization, the data of catalysts **1a**–**c** have been fitted either leaving the $\bar{k}^{c.ep.}$ parameter free or constraining it to zero. The similar χ_r^2 ranges (Table 1) obtained in the two cases prevent one from assessing the presence of the chain epimerization reaction. In effect, the best fit value of the $\bar{k}^{c.ep.}$ parameter turns out to be rather small ($\bar{k}^{c.ep.} < 0.02$), and the profile [*r*] vs [M] is very similar to that obtainable constraining $\bar{k}^{c.ep.}$ to zero (top of Figures 1 and 2).

The fitting results indicate that the enantioselectivity is paractically independent from the substituent R ($\sigma \simeq 0.99$), while this is not the case for the ratio $\bar{k}^{s.ep.}$ between site epimerization and propagation constant.

In the case of the two-parameter fit, the residuals of the computation of pentads at all five concentrations have been reported against pentads (bottom of Figures 1 and 2). In our opinion, this graphical visualization of errors gives a more direct insight into the fit quality respect to crowded numerical tables.

In effect, by inspection of the figures and from the numerical values reported in Table 1, it can be said that the quality of the fits is good for catalysts **1a** and **1c**, and considerably worse for catalyst **1b**. Figure 2 reveals that the disagreement can be ascribed to the *rrrr* pentad alone.

The misfit could be caused by a more complicated catalytic mechanism (more than one kind of active site or a different kinetic scheme due to the prochirality of

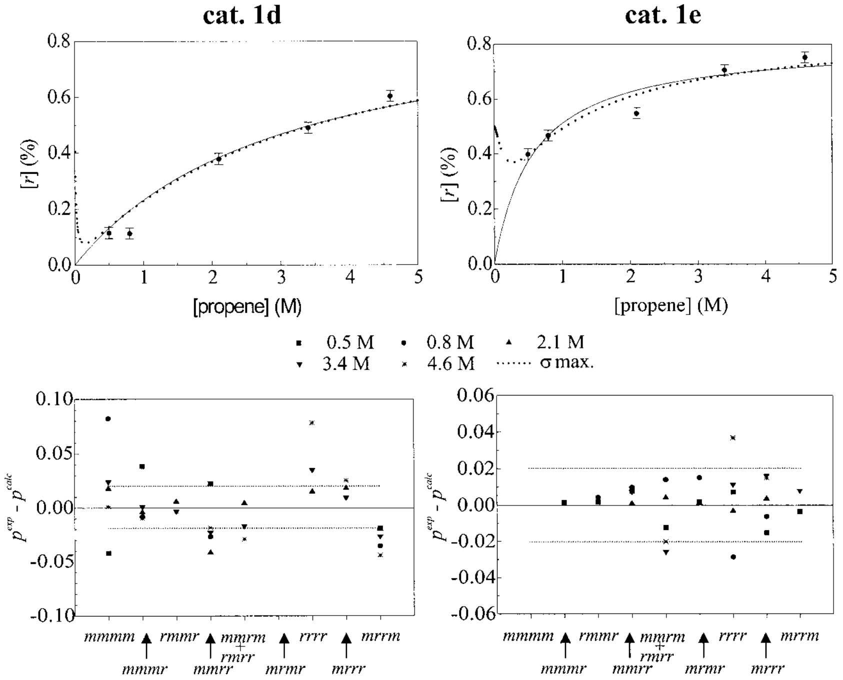

Figure 3. Top: plots of the theoretical dependence of the percentage of the *r* dyad upon monomer concentration for catalysts **1d**,**e**. The continuous and dotted line correspond, respectively, to zero and nonzero rate constant of chain epimerization $k_1^{c.ep.}$ (last and next to last row of parameters in Table 2). The experimental points and the error bars[48] have been derived from ref 16. Bottom: plots of residuals obtained by fitting with two-parameter models the experimental percentages of pentads retrieved by the ^{13}C NMR analysis of five polypropylene samples produced by the C_1-symmetric catalysts **1d**,**e** operated at five different monomer concentrations[16] (see Table 2). Two and three-parameter fits were considered for catalysts **1d** and **1e**, respectively.

the R group of catalyst **1b**). However an analysis of this point is out of the scope of this paper.

***C_1*-Symmetric Systems.** The main fitting results obtained for the two C_1-symmetric catalysts are reported in Table 2.

Leaving as adjustable parameters all the six ratios of kinetic constants, the dissymmetry of both catalysts **1d** and **1e** becomes apparent. Indeed, for a concentration of propene of 1 mol L^{-1}, when the chain occupies position 1, the propagation reaction is preferred with respect to site epimerization ($\bar{k}_1^{\text{s.ep.}} < 1$), while when the chain occupies position 2, the reverse occurs ($\bar{k}_2^{\text{s.ep.}} > 1$). Moreover, the two positions have opposite enantioselectivities.

The numerical values of the best-fit parameters suggest some simplification of the kinetic model. Indeed, within experimental accuracy, $\bar{k}_1^{\text{s.ep.}}$ and $\bar{k}_2^{\text{s.ep.}}$ are found to be 0 and σ_1 is found to be 1. Thus, we fit the data according to a three-parameter model resulting in roughly the same χ_r^2 value.

Moreover, for catalyst **1d**, even the value of $\bar{k}_1^{\text{c.ep.}}$ was found to be zero within experimental accuracy. We thus considered a model with only two parameters. As for C_s-symmetric systems, the complete neglect of chain epimerization does not lead to great changes in the fit (Figure 3). However, in the case of catalyst **1e**, the best fit value of the $\bar{k}^{\text{c.ep.}}$ turns out to be well-defined, and it seems probable that when the chain is coordinated in the more frequently occupied and less hindered position 1, some events of chain epimerization can occur. Moreover the value determined here for $\bar{k}_1^{\text{c.ep.}}$ at 25 °C for catalyst **1e** compares well with the value first obtained for $\bar{k}^{\text{c.ep.}}$ in the case of a C_2-symmetric catalyst: $\bar{k}^{\text{c.ep.}} = 0.05$ M at 30 °C.[23]

The quality of the fits of the final models is rather good in the case of catalyst **1e** and considerably worse in the case of catalyst **1d**, as can be seen from Figure 2 and from the estimated χ_r^2 ranges.

Although the kinetic scheme discussed is nowadays a standard one in organometallic chemistry, it is important to recognize that the connection between microstructure and kinetics developed here has allowed us to test the model and to determine the ratios of its kinetic constants, thus leading to a quantitative description of the mechanism.

Conclusions

We think that the above general connection between microstructure and kinetics in the case of stationary irreversible polymerizations can help considerably in kinetic studies of rather complicated (co)polymerization reactions.

In practice, when one is looking for an experimental confirmation of a kinetic model, is trying to select a model among a finite set of models, or is interested in the quantitative determination of some ratios of kinetic constants, the following method can be adopted.

1. Clear definition of the kinetic models and their translation in terms of the evolution matrix **W**, eq 3.
2. Computation of the transition matrix $\bar{\mathbf{T}} = -(\mathbf{W}^{\text{int}})^{-1}\mathbf{W}^{\text{gr}}$ in the space of kinetic states, starting from a trial set of kinetic parameters.
3. Computation of the percentages expected for the observed sequences according to the model investigated, eq 10.
4. Determination of the best-fit kinetic parameters by minimization of the reduced chi-squared test (eq 11), and comparison of the models investigated.

The application of this protocol to a set of pentad data obtained from C_s and C_1-symmetric doubly bridged metallocenes has offered a quantitative insight in the kinetic mechanism, allowing to determine ratios of kinetic constants ($\bar{k}_x^{\text{s.ep.}}$ and $\bar{k}_x^{\text{c.ep.}}$) which were inaccessible to the stochastic treatment[16,24,25] used so far. Indeed it was possible to express a couple of known stochastic parameters in terms of kinetic constants and monomer concentration, eqs 13−15.

The accessibility of new ratios of kinetic constants opens the way to the evaluation of differences of activation energies and preexponential factors. This topic will be addressed in future works.

Acknowledgment. The author is thankful to Profs. V. Busico and M. Vacatello of the University of Naples for stimulating the work and to Profs. A. Peluso, G. Guerra, and L. Oliva of the University of Salerno for precious discussion and comments.

Appendix

The use of a convenient $\boldsymbol{\tau}$ matrix, as described in the second section of the paper and the definitions in eq 12, allow us to translate the scheme of Figure 1 in the following submatrices of the evolution matrix 3:

$$\mathbf{W}^{int} = \begin{array}{c|cc} & \{R\bullet^n\} & \{S\bullet^n\} \\ \hline \{R\bullet^n\} & \mathbf{W}^{int}_{\bullet} & \mathbf{0} \\ \{S\bullet^n\} & \mathbf{0} & \mathbf{W}^{int}_{\bullet} \end{array}$$

$$\mathbf{W}^{gr} = \begin{array}{c|cc} & \{R\bullet^{n+1}\} & \{S\bullet^{n+1}\} \\ \hline \{R\bullet^n\} & \mathbf{W}(\bullet \to R) & \mathbf{W}(\bullet \to S) \\ \{S\bullet^n\} & \mathbf{W}(\bullet \to R) & \mathbf{W}(\bullet \to S) \end{array}$$

with

$$\mathbf{W}^{int}_{\bullet} = \begin{array}{c|cc} & \{1^n\} & \{2^n\} \\ \hline \{1^n\} & \mathbf{W}^{int}_1 & p_1^{s.ep.}\mathbf{I} \\ \{2^n\} & p_2^{s.ep.}\mathbf{I} & \mathbf{W}^{int}_2 \end{array}, \qquad \mathbf{W}^{int}_i = \begin{array}{c|cc} & R^n_x & S^n_x \\ \hline R^n_x & -1 & p_x^{c.ep} \\ S^n_x & p_x^{c.ep} & -1 \end{array}$$

$$\mathbf{W}(\bullet \to R) = \begin{array}{c|cc} & \{1^{n+1}\} & \{2^{n+1}\} \\ \hline \{1^n\} & \mathbf{0} & \mathbf{I}_1\mathbf{W}^{gr}_{1\to 2} \\ \{2^n\} & \mathbf{I}_1\mathbf{W}^{gr}_{2\to 1} & \mathbf{0} \end{array}$$

$$\mathbf{W}(\bullet \to S) = \begin{array}{c|cc} & \{1^{n+1}\} & \{2^{n+1}\} \\ \hline \{1^n\} & \mathbf{0} & \mathbf{I}_2\mathbf{W}^{gr}_{1\to 2} \\ \{2^n\} & \mathbf{I}_2\mathbf{W}^{gr}_{2\to 1} & \mathbf{0} \end{array}$$

$$\mathbf{I}_1 = \begin{bmatrix} 1 & 0 \\ 0 & 0 \end{bmatrix}, \mathbf{I}_2 = \begin{bmatrix} 0 & 0 \\ 0 & 1 \end{bmatrix}, \mathbf{I} = \mathbf{I}_1 + \mathbf{I}_2$$

$$\mathbf{W}^{gr}_{x\to y} = p_x^p \mathbf{M0} = p_x^p \begin{bmatrix} \sigma_x & 1-\sigma_x \\ \sigma_x & 1-\sigma_x \end{bmatrix}$$

where $p_x^{\text{c.ep.}} = \bar{k}_x^{\text{c.ep.}}/\delta_x$, $p_x^{\text{s.ep.}} = \bar{k}_x^{\text{s.ep.}}/\delta_x$, $p_x^{\text{p}} = [M]/\delta_x$, and $\delta_x = \bar{k}_x^{\text{c.ep.}} + \bar{k}_x^{\text{s.ep.}} + [M]$, with $x,y = 1, 2$.

The stochastic matrix on the kinetic states turns out to be

$$\overline{\mathbf{T}} = -\begin{array}{c|cc} & R\bullet^{n+1} & S\bullet^{n+1} \\ \hline R\bullet^{n} & (\mathbf{W}_{\bullet}^{int})^{-1}\mathbf{W}(\bullet \to R) & (\mathbf{W}_{\bullet}^{int})^{-1}\mathbf{W}(\bullet \to S) \\ S\bullet^{n} & (\mathbf{W}_{\bullet}^{int})^{-1}\mathbf{W}(\bullet \to R) & (\mathbf{W}_{\bullet}^{int})^{-1}\mathbf{W}(\bullet \to S) \end{array} \tag{16}$$

The inversion is easily performed numerically. However its analytical expression is readily obtained as

$$(\mathbf{W}_{\bullet}^{\mathrm{int}})^{-1}\begin{bmatrix} \mathbf{\Delta}^{-1} & 0 \\ 0 & \mathbf{\Delta}^{-1} \end{bmatrix}\begin{bmatrix} \mathbf{W}_2^{\mathrm{int}} & -p_1^{\mathrm{s.ep.}}\mathbf{I} \\ -p_2^{\mathrm{s.ep.}}\mathbf{I} & \mathbf{W}_1^{\mathrm{int}} \end{bmatrix}$$

where $\mathbf{\Delta} = [\mathbf{W}_1^{\mathrm{int}}\ \mathbf{W}_2^{\mathrm{int}} - p_1^{\mathrm{s.ep.}}\ p_2^{\mathrm{s.ep.}}\mathbf{I}]$.

Once the row vector $\mathbf{p}^{\infty} = \lim_{n\to\infty}{}^{1}/_{8}\mathbf{J}\overline{\mathbf{T}}^{n}$ of stationary probabilities has been obtained, the fractional abundance of any given sequence (expressed as usual in the Bovey *m*/*r* notation[20,46]) can be readily computed, using the matrices

$$\overline{\mathbf{T}}_m = \begin{array}{c|cc} & R\bullet^{n+1} & S\bullet^{n+1} \\ \hline R\bullet^{n} & (\mathbf{W}_{\bullet}^{int})^{-1}\mathbf{W}(\bullet \to R) & 0 \\ S\bullet^{n} & \mathbf{0} & (\mathbf{W}_{\bullet}^{int})^{-1}\mathbf{W}(\bullet \to S) \end{array} \tag{17}$$

$$\overline{\mathbf{T}}_r = \begin{array}{c|cc} & R\bullet^{n+1} & S\bullet^{n+1} \\ \hline R\bullet^{n} & 0 & (\mathbf{W}_{\bullet}^{int})^{-1}\mathbf{W}(\bullet \to S) \\ S\bullet^{n} & (\mathbf{W}_{\bullet}^{int})^{-1}\mathbf{W}(\bullet \to R) & \mathbf{0} \end{array} \tag{18}$$

Thus, as a generalization of the method published in ref 25, the fractional abundance of the *mrrm* sequence will be given by $\mathbf{p}^{\infty}\overline{\mathbf{T}}_m\overline{\mathbf{T}}_r\overline{\mathbf{T}}_r\overline{\mathbf{T}}_m\mathbf{J}^T$.

The preceding expressions can be easily simplified in less complicated cases.

If the reaction of epimerization can be neglected, the kinetic states can be reduced to $\{R_1^x, S_1^x, R_2^x, S_2^x\}$ and $\mathbf{W}_1^{\mathrm{int}} = \mathbf{W}_2^{\mathrm{int}} = -\mathbf{I}$. The transition matrix can be obtained from the more general one, eq 16, summing over the *R* and *S* states, yielding

$$\begin{aligned} \overline{\mathbf{T}} &= -(\mathbf{W}_{\bullet}^{\mathrm{int}})^{-1}[\mathbf{W}(\bullet \to R) + \mathbf{W}(\bullet \to S)] \\ &= -(\mathbf{W}_{\bullet}^{\mathrm{int}})^{-1}\mathbf{W}_{\bullet}^{\mathrm{gr}} = \begin{bmatrix} p_1^{\mathrm{s.ep.}}\Delta^{-1}\mathbf{W}_{2\to 1}^{\mathrm{gr}} & \Delta^{-1}\mathbf{W}_{1\to 2}^{\mathrm{gr}} \\ \Delta^{-1}\mathbf{W}_{2\to 1}^{\mathrm{gr}} & p_2^{\mathrm{s.ep.}}\Delta^{-1}\mathbf{W}_{1\to 2}^{\mathrm{gr}} \end{bmatrix} \\ &= \begin{bmatrix} (1 - P_{12})\mathbf{M0}_1 & P_{12}\,\mathbf{M0}_2 \\ P_{21}\mathbf{M0}_1 & (1 - P_{21})\mathbf{M0}_2 \end{bmatrix} \end{aligned} \tag{19}$$

where

$$\mathbf{W}_{\bullet}^{gr} = \begin{array}{c|cc} & \{1^{n+1}\} & \{2^{n+1}\} \\ \hline \{1^{n}\} & \mathbf{0} & \mathbf{W}_{1\to 2}^{gr} \\ \{2^{n}\} & \mathbf{W}_{2\to 1}^{gr} & \mathbf{0} \end{array}$$

$\mathbf{\Delta}^{-1} = (1 - p_1^{\mathrm{s.ep.}}\ p_2^{\mathrm{s.ep.}})^{-1}\mathbf{I}$ and the stochastic parameters P_{12} (P_{21}) give the probability that monomer insertion occurs at site 2 (1) after a previous insertion at site 1 (2).

The last form of the stochastic matrix 19 has been first introduced in ref 25. The advantage of the present kinetic treatment consists in the possibility of giving a kinetic interpretation of the stochastic parameters P_{12} and P_{21}. Indeed introducing the expressions of $\mathbf{\Delta}^{-1}$ and $\mathbf{W}_{x\to y}^{\mathrm{gr}}$ in the last two expressions of eq 19, one gets eq 13:

$$1 - P_{x\neq y} = \frac{p_x^{\mathrm{s.ep.}}\ p_y^{\mathrm{p}}}{(1 - p_1^{\mathrm{s.ep.}}\ p_2^{\mathrm{s.ep.}})} = \frac{\bar{k}_x^{\mathrm{s.ep.}}}{\bar{k}_1^{\mathrm{s.ep.}} + \bar{k}_2^{\mathrm{s.ep.}} + [M]}$$

References and Notes

(1) In a linear (co)polymerization, the monomer(s) A, B, ..., Z join together generating a linear chain composed by different units, A_1, A_2, ..., A_a, B_1, B_2, ..., B_b, ..., Z_1, Z_2, ..., Z_z. According to the IUPAC nomenclature, an irregular polymer, i.e., a polymer composed by different units A_1, A_2, ..., A_M derived from a single monomer A, can be addressed to as a pseudo-copolymer.[2] In effect, although in the kinetic study of a true copolymerization one has the additional degree(s) of freedom of the relative ratio(s) of monomer concentrations in the feed, as far as the description of the polymeric chain is concerned, an irregular polymer presents just the same problems of a copolymer.

(2) Jenkins, A. D.; Kratochvìl, P.; Stepto, R. F. T.; Suter, U. W. *Pure Appl. Chem.* **1996**, *68*, 2287−2311.

(3) Bovey, F. A.; Mirau, P. A. In *NMR of Polymers*; Academic Press: San Diego, CA, 1996; Chapter 2.

(4) Hu, X.; Yan, D. *Makromol. Chem., Theory Simul.* **1992**, *1*, 161−171.

(5) Nele, M.; Collins, S.; Pinto, J. C.; Diaz, M.; Lin, S.; Waymouth, R. M. *Macromolecules* **2000**, *33*, 7294.

(6) Price, F. P. In *Markov chains and Monte Carlo calculations in polymer chains*; Lowry, G. G., Ed; Marcel Dekker: New York, 1970; Chapter 7.

(7) Randall, J. C. *Macromolecules* **1997**, *30*, 803.

(8) Collette, J. W.; Ovenall, D. W.; Buck, W. H.; Ferguson, R. C. *Macromolecules* **1989**, *22*, 3858−3866.

(9) van der Burg, M. W.; Chadwick, J. C.; Sudmeijer, O.;Tulleken, H. J. A. F. *Makromol. Chem., Theory Simul.* **1993**, *2*, 399−420.

(10) Brintzinger, H. H.; Fischer, D.; Mulhaupt, R.; Rieger, B.;Waymouth, R. *Angew. Chem., Int. Ed. Engl.* **1995**, *107*, 1255−1283.

(11) Resconi, L.; Cavallo, L.; Fait, A.; Piemontesi, F. *Chem. Rev.* **2000**, *100*, 1253−1345.

(12) Coates, G. W.; Waymouth, R. M. *Science* **1995**, *267*, 217−219.

(13) Tonelli, A. E. In *NMR Spectroscopy and Polymer Microstructure: The Conformational Connection*; VCH Publishers: New York, 1989.

(14) Busico, V.; Cipullo, R.; Monaco, G.; Vacatello, M.; Segre, A. L. *Macromolecules* **1998**, *31*, 8713−8719.

(15) Angermund, K.; Fink, G.; Jensen, V. R.; Kleinschmidt, R. *Chem. Rev.* **2000**, *100*, 1457−1470.

(16) Veghini, D.; Henling, L. M.; Burkhardt, T. J.; Bercaw, J. E. *J. Am. Chem. Soc.* **1999**, *121*, 564−573.

(17) Reinert, G.; Schbath, S.; Waterman, M. S. *J. Comput. Biol.* **2000**, *7*, 1−46.

(18) Feller, W. In *An introduction to probability theory and its applications*; John Wiley: New York, 1967.

(19) van Kampen, N. G. In *Stochastic processes in physics and chemistry*, North-Holland: Amsterdam, 1987; Chapters 4−5.

(20) Bowden, H. J. In *Macromolecules: an Introduction to Polymer Science*, Bovey, F. A.; Winslow, F. H.; Eds.; Academic Press: New York, 1979; p 129ff.

(21) Ewen, J. A.; Jones, R. L.; Razavi, A.; Ferrara, J. D. *J. Am. Chem. Soc.* **1988**, *110*, 6255−6.

(22) Rieger, B.; Jany, G.; Fawzi, R.; Steimann, M. *Organometallics* **1994**, *13*, 647−653.

(23) Busico, V.; Brita, D.; Caporaso, L.; Cipullo, R.; Vacatello, M. *Macromolecules* **1997**, *30*, 3971−3977.

(24) Farina, M.; Di Silvestro, G.; Sozzani, P. *Macromolecules* **1993**, *26*, 946.

(25) Busico, V.; Cipullo, R.; Corradini, P.; Landriani, L.; Vacatello, M.; Segre, A. L. *Macromolecules* **1995**, *28*, 1887.

(26) Mayo, F. R.; Lewis, F. M. *J. Am. Chem. Soc.* **1944**, *66*, 1594.

(27) Merz, E.; Alfrey, T.; Goldfinger, G. *J. Polym. Sci.* **1946**, *1*, 75.

(28) In the more general case, a kinetic state can be indicated by *m* units of which only the last *L* can rearrange. To have a connection with microstructure, it is necessary that $m \geq L + 1$; in fact rearrangements ($U_i^{n-(L+1)}\ U_j^{n-L}\ \ldots\ U_k^{n-1}\ U_l^{n}$ − catalyst → $U_i^{n-(L+1)}\ U_{j'}^{n-L}\ \ldots\ U_{k'}^{n-1}\ U_{l'}^{n}$ − catalyst) imply that, in an *n*-unit growing chain, unit $U_i^{n-(L+1)}$ is definitively established, but this is not the case of unit U_j^{n-L}, which will be fixed only after the insertion of the $(n + 1)$th monomer.

(29) Doi, Y. *Makromol. Chem., Rapid. Commun.* **1982**, *3*, 635.

(30) Coleman, B. D.; Fox, T. G *J. Chem. Phys.* **1963**, *38*, 1065−1075.

(31) Bovey, F. A.; Tiers, G. V. D. *J. Polym. Sci.* **1960**, *44*, 173−182.

(32) Izzo, L.; Caporaso, L.; Senatore, G.; Oliva, L. *Macomolecules* **1999**, *32*, 6913. Izzo, L.; De Riccardis, F.; Alfano, C.; Caporaso, L.; Oliva, L. *Macomolecules* **2001**, *34*, 2−4.

(33) Prigogine, I.; Nicolis, G. In *Exploring Complexity*; Freeman, W. H.: San Francisco, CA, 1989.

(34) Coleman, B. D.; Fox, T. G *J. Polym. Sci.* **1963**, *1*, 3183−3197.

(35) Cover, T. M.; Thomas, J. A. In *Elements of information theory*; Wiley: New York, 1991; p 69.

(36) Cahn, R. S.; Ingold, C.; Prelog, V. *Angew. Chem., Int. Ed. Engl.* **1966**, *5*, 385.

(37) Lohrenz, J. C. W.; Woo, T. K.; Ziegler, T. *J. Am.Chem. Soc.* **1995**, *117*, 12793−12800.

(38) Yoshida, T.; Koga, N.; Morokuma, K. *Organometallics* **1995**, *14*, 746.

(39) Jensen, V. R.; Borve, K. J.; Ystenes, M. *J. Am. Chem. Soc.* **1995**, *117*, 4109.

(40) Woo, T. K.; Margl, P.; Ziegler, T. *Organometallics* **1997**, *16*, 3454.

(41) Arlman, E. J.; Cossee, P. *J. Catal.* **1964**, *3*, 99.

(42) Grisi, F.; Longo, P.; Zambelli, A.; Ewen, J. A. *J. Mol. Catal. A* **1999**, *140*, 225−233.

(43) Shelden, R. A.; Fueno, T.; Tsunetsugu, T.; Furukawa, J. *Polym. Lett.* **1965**, *3*, 23−26.

(44) Dietrich, U.; Hackmann, M.; Rieger, B.; Klinga, M.; Leskela, M. *J. Am. Chem. Soc.* **1999**, *121*, 4348−4355.

(45) Guerra, G.; Cavallo, L.; Moscardi, G.; Vacatello, M.; Corradini, P. *Macromolecules* **1996**, *29*, 4834.

(46) Frisch, H. L.; Mallows, C. L.; Bovey, F. A. *J. Chem. Phys.* **1966**, *45*, 1565.

(47) Busico, V.; Cipullo, R.; Monaco, G.; Talarico, G.; Vacatello, M.; Chadwick, J. C.; Segre, A. L.; Sudmeijer, O. *Macromolecules* **1999**, *32*, 4173.

(48) Considering the declared reproducibility to be equal to the statistical uncertainty $\sigma(r)$, we can expect the statistical uncertainty σ on any pentad to be smaller than $\sigma(r)$, and thus a lower bound to the χ_r^2 can be obtained assigning to each pentad the same uncertainty $\sigma = \sigma(r) = 0.02$. The estimation of an upper bound for χ_r^2, which corresponds to a lower bound for errors, is more problematic. One can consider the limiting case of a perfectly integrated spectrum, i.e., a spectrum devoid of any instrumental problems and, more importantly, not plagued by the systematic errors coming from overlap. In such a case the errors σ_i should be mainly dictated by the noise and by the chemical reproducibility, mainly associated to temperature and monomer concentration control. The noise contribution is often small, and due to the similar integration interval of the pentad peaks, it is almost constant for all peaks. The chemical contribution to the individual errors is rather difficult to evaluate. However, if one assumes that also these errors are constant, and expressing the percentage of the *r* dyad in terms of the *mr*- and *rr*-centered pentads, one obtains $\sigma = \sigma(r)/\sqrt{3+3/4} \simeq 0.01$.

MA002044Y